A Motion Planning and Tracking Framework for Autonomous Vehicles Based on Artificial Potential Field-Elaborated Resistance Network (APFE-RN) Approach

Yanjun Huang, Haitao Ding, Yubiao Zhang, Hong Wang, Dongpu Cao, Nan Xu, Chuan Hu

***Abstract*—This paper presents a novel motion-planning and tracking framework for automated vehicles based on Artificial Potential Field-Elaborated Resistance (APFE-RN) approach. Motion planning is one of the key parts of autonomous driving, which plans a sequence of movement states to help vehicles drive safely, comfortably, economically, human-like, etc. In this study, the APF method is used to assign different potential functions to different obstacles and road boundaries; while the drivable area is meshed and assigned resistance values in each edge based on the potential functions. A local current comparison method (LCCM) is employed to find a collision-free path. As opposed to a path, the vehicle motion or trajectory should be planned spatiotemporally. Therefore, the entire planning process is divided into two spaces, namely the virtual and actual. In the virtual space, the vehicle trajectory is predicted and executed step by step over a short horizon with the current vehicle speed. Then, the predicted trajectory is evaluated to decide if the speed should be kept or changed. Finally, it will be sent to the actual space, where an experimentally validated Carsim model controlled by a model predictive controller is used to track the planned trajectory. Several case studies are presented to demonstrate the effectiveness of the proposed framework.**

***Index Terms*—Autonomous vehicle, resistance network, motion planning, model predictive controller, obstacle avoidance.**

Manuscript received Month 08, 2018; revised Month 12, 2018; accepted Month 1, 2019. This work was supported by the National Natural Science Foundation of China (U1864206) and Foundation of State Key Laboratory of Automotive Simulation and Control (20170103).

Y. Huang, H. Ding (Corresponding Author:+8613504410291), and N. Xu are with the State Key Laboratory of Automotive Simulation and Control, Jilin University, Changchun, Jilin, China, (e-mail: huangyanjun404@gmail.com;dinght@jlu.edu.cn;xu.nan0612@gmail.com).

Y. Huang, Y. Zhang, H. Wang, and D. Cao are with Department of Mechanical and Mechatronics Engineering, University of Waterloo, Waterloo, ON, Canada, N2L3G1 (gary.zhang@uwaterloo.ca; wanghongbit@gmail.com; dongpu.cao@uwaterloo.ca).

C. Hu is with Department of Mechanical Engineering, University of Texas at Austin, Austin, USA (chuan.hu.2013@gmail.com).

I. INTRODUCTION

AUTONOMOUS vehicles are experiencing substantial advances in academia, industry, and military involving many domains, such as engineering, computer science, and information technology. The most important reason is that autonomous vehicles are capable of alleviating the issues such as road accidents or traffic congestions. Although the idea of autonomous vehicles arose almost a century ago, it did not become true until the 1980s [1], when the PROMETHEUS project was launched.

Advancements in both related hardware and software technologies in the last several decades have further stimulated the interests in autonomous vehicles and many achievements have been made [2][3][4]. For instance, as a milestone in autonomous vehicle technology, a series of DARPA Grand Challenge was held from 2004. The challenges were conducted in both off-road (e.g. 2005) and urban settings (e.g. 2007). The teams were from both industry (e.g. General Motors) and academia (e.g. Carnegie Mellon University, Stanford University, and Virginia Tech), all of them with enthusiasms for improving the capabilities of autonomous vehicles [5]. Other competitions or tests have also been carried out as well, such as the Intelligent Vehicle Future Challenges and the Public Road Urban Driverless Car test (PROUD). In terms of the commercial efforts, Tesla's Autopilot system and the Google self-driving car are attracting more attention [6].

According to SAE international standard J3016, six driving automation levels are defined from "no automation" to "full automation". Each level is featured by its exclusive products, such as adaptive cruise control in level 1 and Autopilot in level 2 [7]. From level 3, the system or the car itself starts to percept the driving environment and then decides the actions. Obviously, as the "brain" of autonomous vehicles, the decision layer is one of the most important parts. Fig. 1 shows the general structure of the autonomous vehicle taking the four-wheel drive electric vehicle as an example [8][9], mainly consisting of the perception, data fusion, decision, and control layer [10]. For the detailed explanation of each layer and their connections please refer to [1]. This study only puts the major emphasis on the decision and control layer.

This article has been accepted for publication in a future issue of this journal, but has not been fully edited. Content may change prior to final publication. Citation information: DOI 10.1109/TIE.2019.2898599, IEEE Transactions on Industrial Electronics

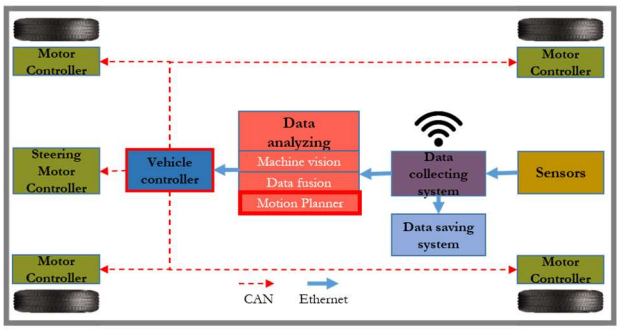

Fig. 1 the structure of an autonomous vehicle

The decision layer is commonly hierarchically structured into global route planning, behavior planning, and local motion planning. At the top level, an autonomous vehicle should decide a route based on passengers' requirement (e.g. the fastest, free of the toll, etc.), the traffic condition, and road network from the current position to the requested destination. A behavior planner aims to reason a sequence of driving behaviors (e.g. turning, stopping, or going straightly) along the planned route according to the current traffic conditions, such as the traffic participants and signals. Whereas, the local motion planning is intended to provide vehicles with a safe (i.e. collision-free and stable), economical, human-like trajectory with a good ride as well as less computational efforts along the predefined route and in accordance with the decided behavior. Given the missions, onboard sensors, and the online sensing information, the global route and the behaviors can be accurately planned [6].

However, more attention and efforts are paid to the local motion planning, and most of them are originated from the mobile robotics. According to the literature, the local motion planning approaches perform in two ways. On one hand, the motion planning is separated spatially and temporally, namely local path planning and velocity planning [11]. On the other hand, the motion should be spatiotemporally planned as a whole. As a traditional path planning methods, Dijkstra's algorithm usually does not carry any velocity information used in the static environment tempting to seek for a collision-free path among static obstacles from the current vehicle location to a temporary terminal location. Generally, numerous studies, such as the geometry-based, grid-based, sampling-based, meta-heuristic-based, artificial potential field (APF) based, and artificial intelligence (AI) based methods are extensively used for path planning or motion planning [12].

In the geometry-based method, reference [13] presents a path generation method using the Voronoi cell algorithm. However, this algorithm only performs well in static rather than dynamic environments and Voronoi edges may be discontinuous and thus unsuitable for the non-holonomic vehicle. In grid-based approaches, an algorithm is proposed in [14] generating maneuvers for high-speed autonomous vehicles over large distances, which is based on Anytime Dynamic A*. Although the solving process is fast, the resulting path is not continuous and it is usually not easy to find the heuristic rule. Sampling-based algorithms are popular in motion planning. A trajectory planning method based on the state-space sampling is studied in [11]. The produced paths connecting the initial state with the sampling terminal states are smooth and kinematic-feasible. However, the method may produce no available path in a dense transportation environment because of very limited state sampling space. Reference [15] presents a motion planning method for autonomous vehicles based on the rapidly-exploring random tree (RRT) algorithm. It can explore the space very quickly; however, the resulted trajectory is suboptimal, jerky and not curvature continuous, which needs further smoothing. Another sampling based method is the state lattice [16][17][18] by discretizing the state space in a deterministic manner. The original version is the nontemporal to deal with the static obstacles and the spatiotemporal state lattices are extended to plan in the presence of moving ones. Whereas, its fidelity and real-time performance depends on the sampling density. It is time-consuming when generating too many trajectory candidates and making individual evaluation of each trajectory. Another effective method is based on meta-heuristic. The authors in [19] provide a motion planning method for mobile robots in uncertain environments based on the genetic algorithm (GA), showing that the result is highly accurate and the robot can respond fast. However, when using GA in autonomous vehicles, the computation complexity is a big trouble for real-time applications. In addition, the classic APF is widely used too. It has advantages in avoiding obstacles in real time; however, the solutions may easily be trapped in the local minima [20]. Recently, the applications of AI-based methods in motion planning are arising. Reference [21] presents an end-to-end system according to the convolutional neural network (CNN), which transforms the camera's raw pixels information directly to steering commands of the autonomous vehicle. It is much more efficient than traditional motion planning techniques and more effective in some scenarios. However, it is hard to collect and train the data from all possible scenarios and the robustness of the system needs to be improved. The path and speed profile are separately planned in [22], where the speed profile is generated by using temporal optimization to optimize all time stamps for the waypoints along the given path. A combined path and speed planner is proposed in [23], which first discretizes both the spatial and temporal space to search the best trajectory according to a set of cost functions. Authors in [24] combine the APF and model predictive control (MPC) to automatically decide its path and velocity in a concise manner.

The control layer, namely motion tracking control, is to guide the vehicle along the planned local trajectory while satisfying some requirements, such as the dynamics stability. In literature [24], the decision and control algorithms are fused together, which makes the formulation more elegant but takes more computational efforts. Because of the limited onboard computational resources, most of the existing research deals with the planning and tracking problem separately in a hierarchical manner [11].

According to the configuration of the studied vehicle (e.g. the type and number of available actuators), numerous control strategies have been extensively studied. Given the common assumption that the tire is purely rolling instead of taking the

slip angle into consideration, a linear matrix inequality (LMI) [25] method is adopted to control a kinematic vehicle model to study how the tire slip angle impacts the closed-loop performance. A model predictive control (MPC) with constraints on both inputs and states is used in [27], which concluded the yaw rate and sideslip angle should also be considered in MPC formulation. Otherwise, the vehicle could fail to accurately track the prescribed path or even became unstable in some extreme conditions. A hierarchical adaptive control is used to address the unknown and non-uniform parameters related to the road condition, where the adaptive law is developed for each wheel [28]. A sliding mode control (SMC) based on chained system theory is developed for path-tracking to attenuate the unmeasurable sliding effects and lateral disturbances [29]. A robust composite nonlinear feedback control is proposed to investigate the path-following performance when the actuation system failures [30][31].

The aforementioned approaches for path or trajectory planning and tracking of autonomous vehicles definitely solve the corresponding problems presented in each literature. However, they are still not applicable because of the computational resources needed (e.g. state-space sampling), complexity (e.g. the separate path and velocity planning as well as the separate planning and control), solution optimality (e.g. graph-based), and heavy training/retraining tasks (e.g. machine-learning based methods). As a result, this paper presents a novel hierarchical planning framework to achieve a balance between these criteria. This study for the first time proposes a local motion-planning and tracking framework for autonomous vehicles based on the resistance network and artificial potential functions. Due to the non-holonomic feature of the autonomous ground vehicle, the grid size or shape should be rearranged. In addition, like the classic grid or graph based path planning methods, the proposed method based on resistance network originally works well in the environment with static obstacles. In other words, the velocity information is not considered when the path is planned. To address this issue, the path planning is repeated temporally in the prediction horizon with the current states and to check if a feasible local trajectory exists. Otherwise, the velocity should be regulated or adapted. By using the proposed resistance-network algorithm, the whole process is speeded up compared to the current grid-based algorithms. The grid is constructed by considering the kinematic constraints of the non-holonomic vehicle. In addition, by using this method, the driver's styles, such as conservative, moderate and aggressive can be included by choosing different grid angle in the kinematic-feasible range. The resulting trajectory is then followed by an experimentally validated Carsim model controlled by an MPC. The feasibility and effectiveness are validated by studying several different cases. More importantly, by adjusting the number of the grid and the prediction horizon length, the methods can be easily used in real time compared to other optimization-based planning methods.

The paper is organized as follows. In Section II, the proposed motion-planning and tracking framework is elaborated step by step from five different aspects. Section III develops an MPC-based trajectory tracker using a bicycle model. Case studies to demonstrate the feasibility of the proposed method are presented in the next section, starting with the demonstration of the experimentally validated Carsim model. Conclusions and the future work are provided in the last section.

II. Motion Planning Framework and Algorithm

In this section, the framework of the local motion planning is designed under the assumption that the ego-vehicle exactly knows the driving environment, the planned global route as well as the behaviors. The proposed method falls into the grid-based category, such that it is applicable in both structured and unstructured driving environment. Simply, all the following work is conducted in a structured road environment. In addition, the assumptions used in this study are as follows:

(1): The perception part is properly working to provide the accurate information of driving environment;

(2): All the vehicles are driving on a structured straight road with two lanes in the driving direction;

(3): The states of the surrounding vehicles are assumed to be unchanged in a short period.

A. Grid Construction

Differing from the mobile robots, the autonomous vehicle cannot drive in any direction due to its non-holonomic characteristics. Therefore, it is not realistic to directly employ the rectangle gird as [33] did. To address this issue, this study proposes a novel meshing method as shown in Fig. 2 by considering vehicle kinematic constraints. Only one longitudinal line is kept per lane to represent the centerline of the lane, which means the longitudinal motion of the vehicle is constrained to drive along the centerline of the current lane.

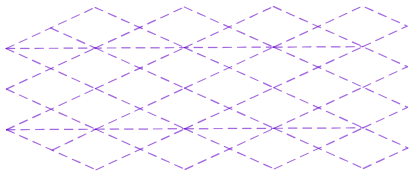

Fig. 2 the proposed grid structure

The process to mesh the feasible driving region ahead of the ego-vehicle is summarized in Table I and shown in Fig. 3.

TABLE I
MESHING PROCESS

1	The global route planner generates a global route or path (e.g. red dot line in Figure 3) according to the structure of the road [32], which is a curve and reflects the curvature of the current road.
2	Assume the planned global route is on the centerline of the lane, based on the number and length of each of the longitudinal grid, several waypoints along the centerline can be defined in the local horizon.
3	For each waypoint, according to the lateral width of the grid, their adjunct points can be assigned along the normal direction through the current waypoint [23].
4	The grid is finally constructed by connecting the nodes as shown in Fig. 3 (d)

The above process is visualized by the Fig. 3. According to the online sensing information of the road architecture, the meshed region in a local horizon is shown in Fig. 4 (a) (straight road) and Fig. 4 (b) (curved road).

This article has been accepted for publication in a future issue of this journal, but has not been fully edited. Content may change prior to final publication. Citation information: DOI 10.1109/TIE.2019.2898599, IEEE Transactions on Industrial Electronics

a b

c d

Fig. 3 the meshing process

a b

Fig. 4 grid in the straight (a) and curved (b) road

B. Grid Dimension Determination

In this section, the geometry dimensions of the grid are determined by taking kinematic constraints into consideration. According to the shape of the grid, the most difficult path is from node 1 to 3 as shown in Fig. 5.

Fig. 5 determination of the grid size

In order to make sure the planned path is feasible in the planning phase, the following equations should hold:

$$a_y = V^2/R \le \lambda g \tag{1}$$

$$tan\theta = b/a \ge R\Big/\sqrt{\left(a^2+b^2\right)} \tag{2}$$

$$b \ge \sqrt{\left(\sqrt{a^4+4\left(aV^2/\lambda g\right)^2}-a^2\right)\Big/2} \tag{3}$$

Constraint (1) is applied to keep the vehicle stable or even make the passengers comfortable when cornering. Commonly λ=0.4. In order to ensure the vehicle is capable of driving from node 1 and passing node 3, constraint (2) should be satisfied. Based on constraints (1) and (2), (3) can be obtained, which shows the correlation between the grid size and the vehicle velocity.

C. Resistance Network Generation

This section elaborates the process of generating the resistance network. Based on the generated grid on a local horizon as shown in Fig. 6, where the road with double lanes is used as an example. This method can be easily extended to other scenarios based on the road structure. A voltage source is added by connecting the starting point (i.e. current vehicle location) and the local terminal point. Each edge will be assigned a resistance value by the APF method. In this way, the currents are produced and flow throughout the whole network. Unlike the classic APF methods [27], in this study, only the obstacles are modeled by potential functions to repulse the vehicle. Two types of potential functions are used to demonstrate the road and obstacles. Different functions can be used to define the road and obstacles, and this paper employs the exponential and parabolic functions as shown in Fig. 7 and [24]. According to the location of the obstacles or adjacent vehicles, the potential functions are generated across the local horizon. The resistance values are therefore acquired for each corresponding middle point of each edge.

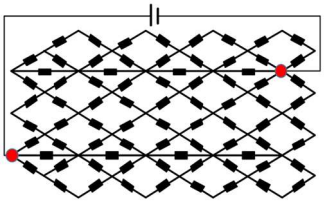

Fig. 6 generated grid in a local horizon

Currently, since the ego-vehicle is still a point, the other objects on the road are enlarged by adding an envelope around each object.

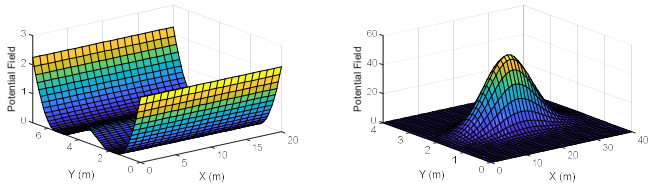

a b

Fig. 7 potential functions for road (a) and obstacles (b)

D. Current Calculation and Path Determination

According to the resistance network shown in Fig. 6, the number of the grid (i.e. triangle and quadrangle), node, and edge are denoted by g, n, and e, satisfying $e = g + n - 1$ [33]. The Kirchhoff current law implies that in an electric network, the sum of currents flowing into any node is identical to the sum of currents flowing out of that node. Based on the current law, a matrix A can be derived with a dimension of $n \times e$. For each entry $A_{ij}, i = 1,2\cdots n; j = 1,2,\cdots e$, its value should be one of the three numbers 1, -1, or 0. 1 and -1 means the current of the edge j flows out of or into the node i; whereas, 0 denotes the disconnection of edge j and the node i. In addition, the Kirchhoff voltage law defines that the algebraic summation of all the voltages around any closed loop in an electrical circuit is zero. As a result, a matric B is obtained with the dimension of $g \times e$. For each entry $B_{ij}, i = 1,2\cdots g; j = 1,2,\cdots e$, its values should also be one of the three numbers 1, -1, or 0. 1 and -1 means the

current of the edge j flow in the direction that is same with the direction of the closed loop; whereas, 0 means the edge j does not belong to the loop i. After assigning resistance values by PFs in the previous section, the resistance matrix R can be defined as:

$$R_{e\times e} = diag\left[R_1, R_2, \cdots R_e\right] \tag{4}$$

The current I and voltage U for all branches in the network are defined by:

$$I_{e\times 1} = \left[i_1, i_2, \cdots i_e\right]^T \tag{5}$$

$$V_{e\times 1} = \left[v_1, v_2, \cdots v_e\right]^T \tag{6}$$

As aforementioned, the following two equations hold:

$$A_{n\times e} I_{e\times 1} = 0 \tag{7}$$

$$B_{g\times e} V_{e\times 1} = 0 \tag{8}$$

Given the voltage of the energy source v_e, based on Ohm's law, the following equation is derived:

$$V_{e\times 1} = R_{e\times e} I_{e\times 1} - \left[0_{(e-1)\times 1}, v_e\right]^T \tag{9}$$

By rearranging the above equations, the current of each edge can be determined by:

$$I_{e\times 1} = \left[A_{(n-1)\times e}, B_{g\times e}\right]^T \backslash \left(B_{g\times e}\left[0_{(e-1)\times 1}, v_e\right]^T\right) \tag{10}$$

Note that for any closed-loop circuit, the rank of a matrix A is $n-1$ such that $A_{(n-1)\times e}$ in (7) is obtained by deleting any row of the matrix $A_{n\times e}$. According to the local current comparison method [34][35], After determination of currents flowing through each edge, the collision-free path is thus selected by following the direction of the local maximum current at each successive node between the starting and terminal nodes.

E. Motion Planning

Until now, the proposed method still belongs to the path planning without reasoning the velocity. However, unlike other path planning methods, the proposed method will figure out a path even when it is not feasible or a collision-free one. To address this problem, the following approach is proposed as shown in Fig. 8, the whole space is divided into two, namely the virtual and the actual.

In the virtual space, the aforementioned planning method will decide the path in each step for totally N steps with the assumption that the environment will maintain the current states. In each step, the ego-vehicle will move one-step forward along the planned path with the current speed. In other words, the ego-vehicle predict its own trajectory in the next N steps. In addition, given a small value N, it is reasonable to assume the other traffic participants keep their own states constant. For example, the car in the left lane will drive at the current speed and stay in its own lane in the virtual space. The whole process results in that a collision-free trajectory either does or does not exist. Fig. 9 shows the case when a collision-free trajectory exists in the virtual space with the current speed, where subfigure a, b, c, indicate the predicted path in dot line at different time step in the virtual space. The subfigure d means the ego-vehicle takes one-step forward in the actual space at the current speed. Whereas, Fig. 10 describes the case when a collision-free trajectory does not exist in the prediction horizon with the current speed. Subfigure presents the predicted path zigzags from the current location to the local terminal. That means the ego-vehicle cannot drive either left or right due to the other participants on both sides. Therefore, it would be unsafe to keep the current speed so that the ego-vehicle deaccelerates in next time instant and then the whole process repeats.

Note: the objective of the velocity plan is to drive at the allowable maximum speed as long as possible.

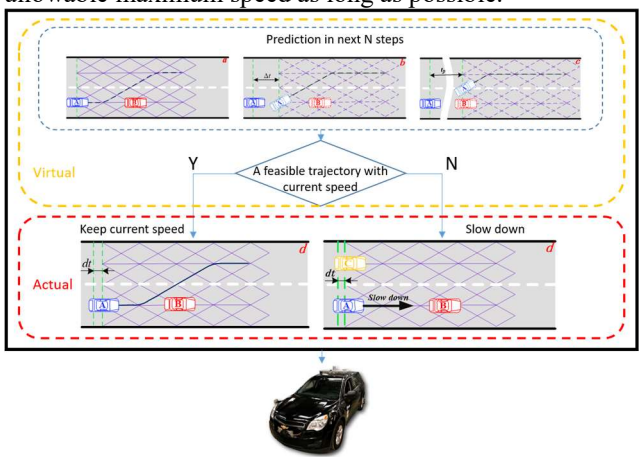

Fig. 8 Structure of proposed motion planning

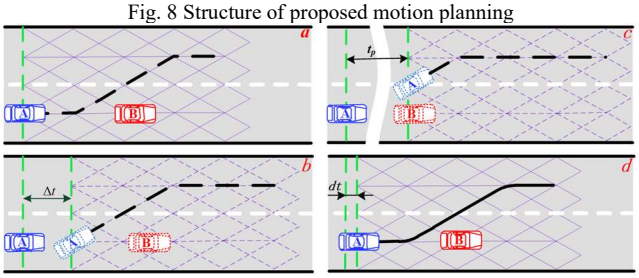

Fig. 9 Demonstration of a feasible trajectory without changing speed

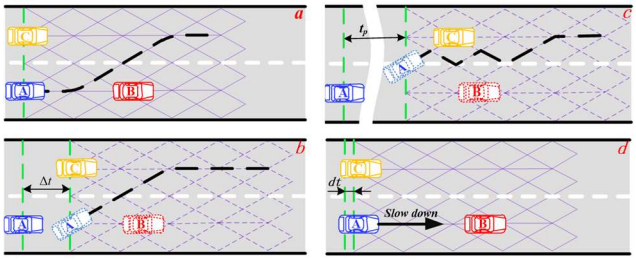

Fig. 10 Demonstration of a non-feasible trajectory without changing speed

III. Motion Tracking Control

In this section, the motion-tracking controller is presented in order to smooth the planned path, which is composed of multiple lines and not curvature-continuous.

A. Vehicle Dynamics Model

The vehicle dynamics is really complicated and high fidelity models are non-linear, discontinuous and computationally expensive. To design the controller, a bicycle model is used. Fig. 11 depicts a diagram of the bicycle model, including the longitudinal, lateral, and yaw degrees of freedom [36][37][38]:

This article has been accepted for publication in a future issue of this journal, but has not been fully edited. Content may change prior to final publication. Citation information: DOI 10.1109/TIE.2019.2898599, IEEE Transactions on Industrial Electronics

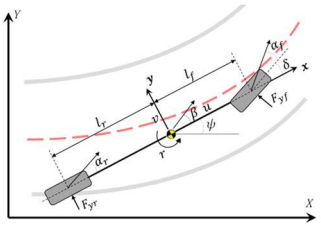

Fig. 11 bicycle model

The model of the bicycle can be shown [24] [39] [40]:

$$m(\dot{u} - vr) = F_{xT} \tag{11}$$

$$m(\dot{v} + ur) = F_{yf} + F_{yr} \tag{12}$$

$$I_z \dot{r} = F_{yf} l_f - F_{yr} l_r \tag{13}$$

The vehicle's motion with respect to global coordinates is:

$$\dot{X} = u\cos\psi - v\sin\psi, \quad \dot{Y} = u\sin\psi + v\cos\psi \tag{14}$$

where, m is the vehicle's mass, and I_z is the vehicle 's moment of inertia about z-axis; l_f /l_r are the distance from CG(center of gravity) to front /rear axle. u, v and r denote the longitudinal velocity, lateral velocity, and yaw rate of the vehicle at CG, X, Y and ψ are the longitudinal and lateral position and heading angle of the vehicle in the global coordinate, F_{yf} and F_{yr} are the total lateral forces of the front and rear tires, F_{xT} is the total longitudinal force of tires.

A linear tire model is used to calculate the lateral forces:

$$F_{yf} = -\bar{C}_{\alpha f}\alpha_f = \bar{C}_{\alpha f}\left(\delta - \frac{v + l_f r}{u}\right) \tag{15}$$

$$F_{yr} = -\bar{C}_{\alpha r}\alpha_r = \bar{C}_{\alpha r}\left(-\frac{v - l_r r}{u}\right) \tag{16}$$

where α_f and α_r denote the sideslip angles of the front and rear tires, and δ is the steering angle. At each instant of time, $\bar{C}_{\alpha f}$ and $\bar{C}_{\alpha r}$ which denote the cornering stiffness of the front and rear tires, are obtained using look-up tables of tire stiffness data, similar to [41].

Synthesizing Equations (11)-(16), the vehicle's operating point dynamic in global coordinates can be written in an LTV state space form as:

$$\dot{\boldsymbol{x}} = \bar{\boldsymbol{A}}\boldsymbol{x} + \bar{\boldsymbol{B}}\boldsymbol{u} \tag{17}$$

$$\boldsymbol{y} = \boldsymbol{C}\boldsymbol{x} \tag{18}$$

where $\boldsymbol{x} = \begin{bmatrix} X & u & Y & v & \psi & r \end{bmatrix}^T$, $\boldsymbol{u} = \begin{bmatrix} F_{xT} & \delta \end{bmatrix}^T$, and the output map $\boldsymbol{y} = \begin{bmatrix} u & Y & \psi \end{bmatrix}^T$.

B. Tracking Controller based on MPC

The path tracking task can be posed as a predictive tracking control problem with constraints. Desired references for the heading angle ψ_d, the lateral position, and the speed u_d are generated and updated in the motion planning. In a model predictive control (MPC) scheme, the model of the plant is used to predict the future evolution of the system, and the controller action sequence is achieved by repeatedly solving finite time optimal control problems in a receding horizon fashion [42] [43][44]. Based on the prediction, at each time step t, an open-loop optimal control problem with a certain or cost function and operating constraints are solved over a finite horizon.

To obtain a finite dimensional optimal control problem, the system dynamics (17) is discretized using the Euler method [45]:

$$\boldsymbol{x}(\boldsymbol{k}) = \bar{\boldsymbol{A}}_{\boldsymbol{d}}\boldsymbol{x}(\boldsymbol{k}) + \bar{\boldsymbol{B}}_{\boldsymbol{d}}\boldsymbol{u}(\boldsymbol{k}) \tag{19}$$

$$\boldsymbol{y}(\boldsymbol{k}) = \boldsymbol{C}_{\boldsymbol{d}}\boldsymbol{x}(\boldsymbol{k}) \tag{20}$$

where $\bar{\boldsymbol{A}}_{\boldsymbol{d}}, \bar{\boldsymbol{B}}_{\boldsymbol{d}}, \boldsymbol{C}_{\boldsymbol{d}}$ are the state matrix, input matrix and output matrix in the augmented form. The control incremental $\Delta\boldsymbol{u}$ is used. i.e., $\boldsymbol{u}(\boldsymbol{k}) = \boldsymbol{u}(\boldsymbol{k}-1) + \Delta\boldsymbol{u}(\boldsymbol{k})$ and $\boldsymbol{u}(\boldsymbol{k}) = \begin{bmatrix} F_{xT}(k) & \delta(k) \end{bmatrix}^T$

The cost function is defined to reflect the control objective:

$$\boldsymbol{J}(\boldsymbol{x}(\boldsymbol{t}), \Delta\boldsymbol{U}_{\boldsymbol{t}}) = \sum_{\boldsymbol{k}=1}^{\boldsymbol{N_p}} \left\| \boldsymbol{y}_{\boldsymbol{t}+\boldsymbol{k},\boldsymbol{t}} - \boldsymbol{y}_{\boldsymbol{d}\ \boldsymbol{t}+\boldsymbol{k},\boldsymbol{t}} \right\|_{\boldsymbol{Q}}^2 + \sum_{\boldsymbol{k}=0}^{\boldsymbol{N_p}-1} \left\| \Delta\boldsymbol{u}_{\boldsymbol{t}+\boldsymbol{k},\boldsymbol{t}} \right\|_{\boldsymbol{R}}^2 \tag{21}$$

where, $\Delta\boldsymbol{U}_{\boldsymbol{t}} \triangleq \left[\Delta\boldsymbol{u}_{\boldsymbol{t},\boldsymbol{t}}, \quad \cdots \quad \Delta\boldsymbol{u}_{\boldsymbol{t}+\boldsymbol{N_p}-1,\boldsymbol{t}} \right]^T$ represents the optimization sequence at time t, and the $\boldsymbol{y}_{\boldsymbol{d}} = \begin{bmatrix} u_d & Y_d & \psi_d \end{bmatrix}^T$ denotes the planned reference signal. Index $\boldsymbol{t}+\boldsymbol{k},\boldsymbol{t}$ denotes the predicted value at $\boldsymbol{k}$ steps ahead of the current time $\boldsymbol{t}$. The first term in (11) is the tracking error of the references from motion planning. The second term is the variations of inputs to penalize the control efforts. The positive semi-definite Q and R are weighting matrices that reflect the importance of these terms in the cost function.

At each time step t the following finite horizon optimal control problem is solved on-line:

$$\min_{\Delta U_t} \quad J(x(t), \Delta U_t) \tag{22}$$

$$\text{s. t.} \quad x_{k+1,t} = \bar{A}_d x_{k,t} + \bar{B}_d \Delta u_{k,t} \tag{22.a}$$

$$y_{k,t} = C_d\, \bar{x}_{k,t} \tag{22.b}$$

$$y_{\min} \le y_{k,t} \le y_{\max} \tag{22.c}$$

$$u_{\min} \le u_{k,t} \le u_{\max} \tag{22.d}$$

$$\Delta u_{\min} \le \Delta u_{k,t} \le \Delta u_{\max} \tag{22.e}$$

$$u_{k,t} = u_{k-1,t} + \Delta u_{k,t} \tag{22.f}$$

$$k = t, \cdots, t + N_p - 1$$

$\Delta\boldsymbol{U}_{\boldsymbol{t}}^{*} \triangleq \left[\Delta\boldsymbol{u}_{\boldsymbol{t},\boldsymbol{t}}^{*}, \quad \cdots \quad \Delta\boldsymbol{u}_{\boldsymbol{t}+\boldsymbol{N_p}-1,\boldsymbol{t}}^{*} \right]^T$ is the sequence of the optimal input increments computed at current time t. Only the first element of the sequence is applied, which results in state feedback control law at the time t:

$$u(t, x(t)) = u(t-1) + \Delta u_{t,t}^{*} \tag{23}$$

There are three types of the constraints in (22), the first one (12c) deals with the output constraint, e.g. the vehicle speed, the lateral position, and the heading angle. The second (12d) and the third one (12e) relate to control constraints. In addition, in order to guarantee the stability of the developed linear time varying MPC, the process according to [26] is followed, where another terminal constraint is employed. The steering angle and total longitudinal force and their rates of change are bounded, due to the actuators limits and vehicle stability. One should note that all the constraints could be transformed to the formulation of $\Delta\boldsymbol{U}_{\boldsymbol{t}}$, details in [27].

This article has been accepted for publication in a future issue of this journal, but has not been fully edited. Content may change prior to final publication. Citation information: DOI 10.1109/TIE.2019.2898599, IEEE Transactions on Industrial Electronics

Remarks: why augmented form? It is well posed and ensures offset-free tracking in the control law while using tracking errors and control increments in the cost function. Incremental models contain an internal disturbance, in which give unbiased predictions in the steady state and prevent unreasonable chatter. [46]. As another issue, one might note that the total longitudinal force (F_{xT}) calculated by tracking controller is actually an upper-level control action, which means virtual. It should be applied via the wheel motors and the brakes. The lower level torque/brake distribution control goes beyond this work and can be referred to [47]. We simply consider the motor torque/ brake torque of each wheel applies a quarter of the force (F_{xT}).

IV. Motion Tracking Control

This section elaborates the test environment and whole simulation procedure.

A. Simulation Setup

The proposed framework is simulated to evaluate its performance. The vehicle of Chevrolet-Equinox shown in Figure 12 is used in CarSim software. The parameters listed in Table 1 are used in the simulation are extracted from this vehicle. To validate the CarSim platform, a double lane change maneuver (with the same steering angle and speed inputs) is performed in the field test and CarSim environment, respectively. The comparative results in Fig. 13 indicate the reliability and accuracy of the simulation environment.

Fig. 12 The studied vehicle is an electric 4WD Chevrolet Equinox.

TABLE II
VEHICLE PARAMETERS

Parameter	Value(units)	Description
m	2270kg	Vehicle mass
l_f	1.421m	Distance from the front axle to CG
l_r	1.434m	Distance from the rear axle to CG
I_z	4600 kgm^2	Yaw moment of inertia
R_{eff}	0.351m	Wheel effective radius

The validation results of the Carsim model are shown in the following figure, where the location, speed, and the yaw rate response during a double-lane-change maneuver are presented.

B. Co-simulation Procedure

In this study, a road with a single lane in each direction is adopted for evaluating the proposed method. It can however be easily extended to other structured/unstructured driving environment.

As shown in Figure 14, at each time step, once the actual driving is accurately perceived, the grid is generated according to the road structure and the current velocity. The resistance network is constructed after assigning resistance in accordance with the obstacles information around the vehicle. The trajectory is planned by the proposed method, which is tracked by the Equinox built in Carsim controlled by an MPC. The process is repeated at a fixed sample rate.

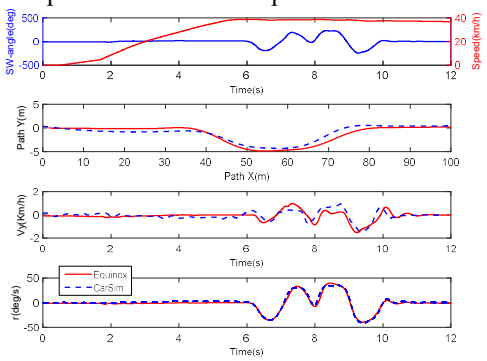

Fig. 13 Carsim model validation

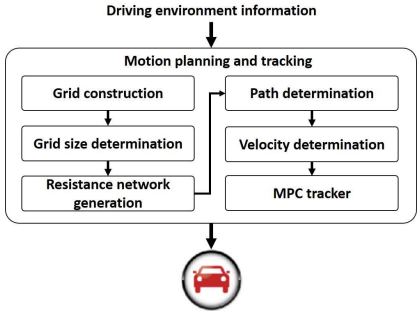

Fig. 14 Co-simulation procedure during each time instant

V. Case Study

In this section, four different cases are studied to demonstrate the feasibility of the proposed methods under different conditions.

A. Case A

In this case, the ego-vehicle is driving at a maximum allowable speed (60km/h); whereas the leading vehicle is moving slowly (50km/h) in the same lane. The initial distance between two vehicles is about 30 m. Fig. 17 indicates the whole process in 10 seconds driving, where the ego-vehicle and leading vehicle are shown in blue and red, respectively.

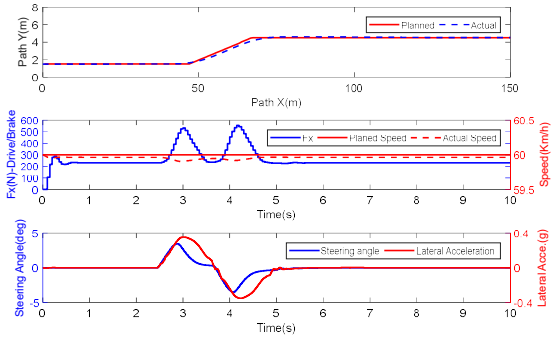

Fig. 15 vehicle responses in case A

The numbers are used to indicate the different time from the initial to the final position. For example, a blue car with number 1 shows the initial position of the ego-vehicle. As it can be seen, when the ego-vehicle is approaching the leading one and in a certain distance, it switches to left and starts to change the lane.

This article has been accepted for publication in a future issue of this journal, but has not been fully edited. Content may change prior to final publication. Citation information: DOI 10.1109/TIE.2019.2898599, IEEE Transactions on Industrial Electronics

Since the target lane is clear, it can successfully achieve the lane-change maneuver to pass the slow vehicle without changing the speed. Fig. 15 present vehicle responses, such as the location, velocity, and lateral acceleration. It can be seen the Carsim model can perfectly track the trajectory controlled by the proposed MPC.

B. Case B

In this case, the ego-vehicle is driving at 60km/h, and the leading vehicle is moving at 50km/h with the initial distance about 30 m in the same lane. In addition, another car is running at 50km/h in the adjacent lane, which is closed to the ego-vehicle. Thus, the ego-vehicle slows down to keep the safe distance as shown in case B of Fig. 17, while Fig. 16 demonstrates the vehicle responses during this scenario.

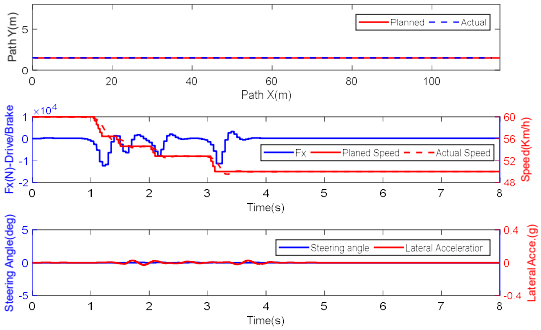

Fig. 16 vehicle responses during case B

C. Case C

This case is very similar to case B with the only difference that the car in the adjacent lane is moving at 60 km/h. In this way, the ego-vehicle starts to slow down and follow the leading vehicle with a safe distance because at the beginning it is not possible to conduct the overtaking maneuver. During this period, the ego-vehicle always decides if there is any feasible trajectory to maintain the maximum speed. When the yellow car in the adjacent lane is driving away at 60km/h, the ego-vehicle is preparing to turn left and pass the leading car. Since the goal is to find the fastest trajectory, the ego-vehicle speeds up when finishing the lane-change maneuver. The vehicle responses during this period are indicated in the following figures.

D. Case D

In this case, the leading vehicle is driving very slowly (e.g. 25km/h) and the vehicle is moving at 50km/h in the adjacent lane. The ego-vehicle is approaching the leading car with the speed 60km/h.

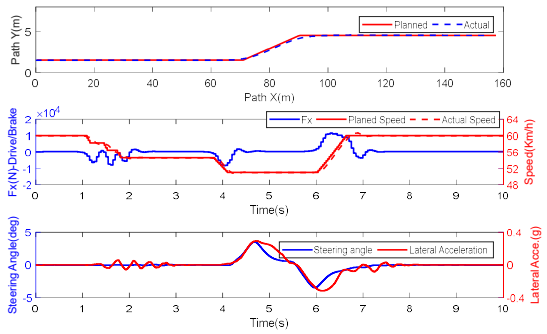

Fig. 18 vehicle responses during case C

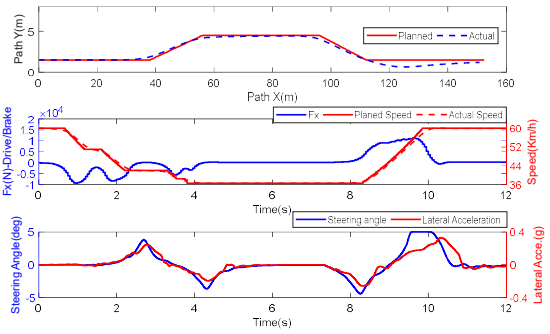

Fig. 19 vehicle responses during case D

It then decreases the speed to maintain a safe longitudinal

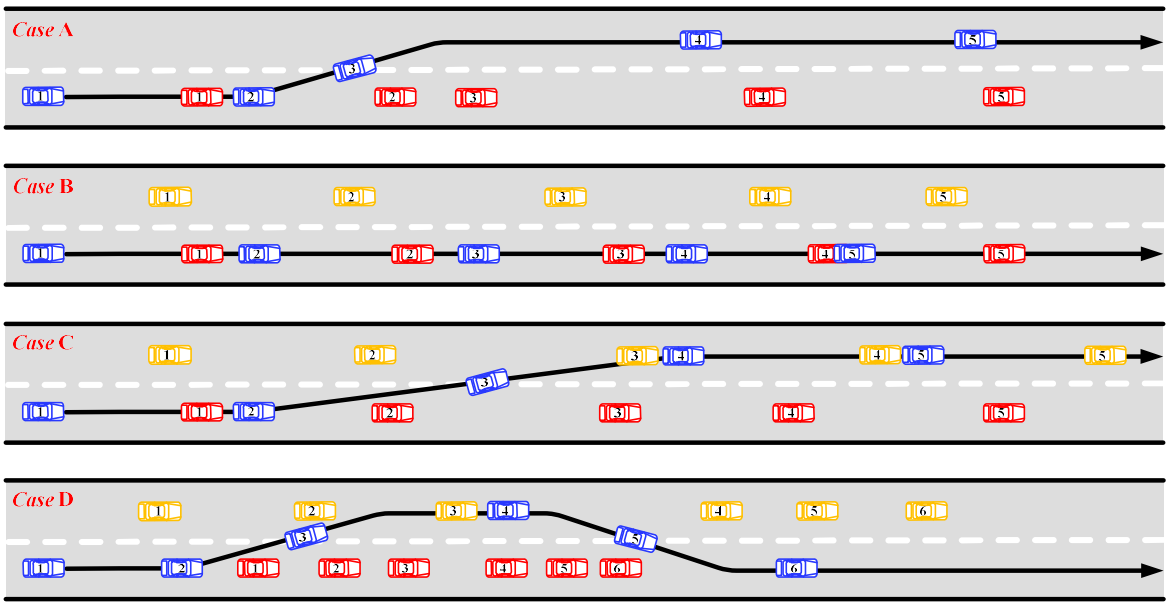

Fig. 17 Demonstration of the vehicle movement for each case

distance with the leading car. When the left lane is clear and has enough space to accommodate the ego-vehicle, it changes the lane and then tries to speed up. In order to keep the high speed, the ego-vehicle turns left and changes the lane. It then tries to speed up to the maximum speed, but the yellow car ahead is still slow and impede the ego-vehicle. Therefore, the ego-vehicle passes the yellow car by returning to the original lane, and finally, it increases the velocity to the maximum.

VI. Conclusion

This paper presented a motion planning and tracking framework by using the resistance network and MPC for autonomous vehicles. Since the classic resistance network only solves the path-planning problem, the velocity is included by predicting the planned path in next several time intervals. Therefore, the proposed method performs like a human driver because it is able to predict and react accordingly. In addition, an experimentally validated Carsim model was used to track the planned trajectory using an MPC. More importantly, different scenarios were studied to demonstrate the feasibility of the proposed method in terms of the automatic decisions on obstacle-avoidance and fastest motion. Further work will be focused on the comparison of different classic motion planning methods to further show the advantages of the proposed method and its experimental validation.

References

[1] E. Dickmanns and V. Graefe, "Dynamic monocular machine vision", Machine Vision and Applications, vol. 1, no. 4, pp. 223-240, 1988.

[2] C. Shen, Y. Shi and B. Buckham, "Path-Following Control of an AUV: A Multiobjective Model Predictive Control Approach", IEEE Transactions on Control Systems Technology, pp. 1-9, 2018.

[3] C. Shen, Y. Shi and B. Buckham, "Integrated Path Planning and Tracking Control of an AUV: A Unified Receding Horizon Optimization Approach", IEEE/ASME Transactions on Mechatronics, vol. 22, no. 3, pp. 1163-1173, 2017.

[4] M. Campbell, M. Egerstedt, J. How, et al, "Autonomous driving in urban environments: approaches, lessons and challenges", Philosophical Transactions of the Royal Society A: Mathematical, Physical and Engineering Sciences, vol. 368, no. 1928, pp. 4649-4672, 2010.

[5] C. Urmson, C. Baker, J. Dolan, P. Rybski, B. Salesky, W. Whittaker, D. Ferguson and M. Darms, "Autonomous Driving in Traffic: Boss and the Urban Challenge", AI Magazine, vol. 30, no. 2, p. 17, 2009.

[6] B. Paden, M. Cap, S. Yong, et al, "A Survey of Motion Planning and Control Techniques for Self-Driving Urban Vehicles", IEEE Transactions on Intelligent Vehicles, vol. 1, no. 1, pp. 33-55, 2016.

[7] Automated driving levels of driving automation are defined in new SAE international standard J3016.

[8] R. Wang, H. Zhang and J. Wang, "Linear Parameter-Varying Controller Design for Four-Wheel Independently Actuated Electric Ground Vehicles With Active Steering Systems," IEEE Transactions on Control Systems Technology, vol. 22, no. 4, pp. 1281-1296, July 2014.

[9] Zhibin Shuai, Hui Zhang, Junmin Wang, Jianqiu Li, Minggao Ouyang, "Lateral motion control for four-wheel-independent-drive electric vehicles using optimal torque allocation and dynamic message priority scheduling," Control Engineering Practice, vol. 24, pp. 55-66, 2014.

[10] D. Gonzalez, J. Perez, V. Milanes and F. Nashashibi, "A Review of Motion Planning Techniques for Automated Vehicles", IEEE Transactions on Intelligent Transportation Systems, vol. 17, no. 4, pp. 1135-1145, 2016.

[11] X. Li, Z. Sun, D. Cao, D. Liu and H. He, "Development of a new integrated local trajectory planning and tracking control framework for autonomous ground vehicles", Mechanical Systems and Signal Processing, vol. 87, pp. 118-137, 2017.

[12] X. Hu, L. Chen, B. Tang, et al, "Dynamic path planning for autonomous driving on various roads with avoidance of static and moving obstacles", Mechanical Systems and Signal Processing, vol. 100, pp. 482-500, 2018.

[13] Lee U, Yoon S, Shim H C, et al, "Local path planning in a complex environment for self-driving car", Cyber Technology in Automation, Control, and Intelligent Systems (CYBER), 2IEEE 4th Annual International Conference on IEEE: 445-450, 2014.

[14] O. Brock, J. Trinkle, F. Ramos, "Planning Long Dynamically-Feasible Maneuvers for Autonomous Vehicles", MIT Press:214-221, 2009.

[15] L. Ma, J. Xue, K. Kawabata, J. Zhu, C. Ma and N. Zheng, "Efficient Sampling-Based Motion Planning for On-Road Autonomous Driving", IEEE Transactions on Intelligent Transportation Systems, vol. 16, no. 4, pp. 1961-1976, 2015.

[16] J. Ziegler and C. Stiller, "Spatiotemporal state lattices for fast trajectory planning in dynamic on-road driving scenarios," in Intelligent Robots and Systems, 2009. IROS 2009. IEEE/RSJ International Conference on, 2009, pp. 1879-1884.

[17] M. McNaughton, C. Urmson, J. M. Dolan, and J.-W. Lee, "Motion planning for autonomous driving with a conformal spatiotemporal lattice," in Robotics and Automation (ICRA), 2011 IEEE International Conference on, 2011, pp. 4889-4895

[18] T. Gu, J. Snider, J. M. Dolan, and J.-w. Lee, "Focused Trajectory Planning for autonomous on-road driving," in Intelligent Vehicles Symposium (IV), 2013 IEEE, 2013, pp. 547-552

[19] R. K. Panda, B. B. Choudhury, "An effective path planning of mobile robot using genetic algorithm", Computational Intelligence & Communication Technology (CICT), International Conference on. IEEE: 287-291, 2015.

[20] H. Bing, L. Gang, G. Jiang, et al, "A route planning method based on improved artificial potential field algorithm", IEEE International Conference on Communication Software and Networks:550-554, 2011.

[21] M. Bojarski, D. Del Testa, D. Dworakowski, et al, "End to end learning for self-driving cars", arXiv preprint arXiv:1604.07316, 2016.

[22] C. Liu, W. Zhan, and M. Tomizuka, "Speed profile planning in dynamic environments via temporal optimization", In Intelligent Vehicles Symposium (IV), IEEE (pp. 154-159), 2017.

[23] W. Xu, J. Wei, J. M. Dolan, et al, "A real-time motion planner with trajectory optimization for autonomous vehicles", In Robotics and Automation (ICRA), IEEE International Conference on (pp. 2061-2067), 2012.

[24] Y. Rasekhipour, A. Khajepour, S. Chen and B. Litkouhi, "A Potential Field-Based Model Predictive Path-Planning Controller for Autonomous Road Vehicles", IEEE Transactions on Intelligent Transportation Systems, vol. 18, no. 5, pp. 1255-1267, 2017.

[25] S. Arogeti and N. Berman, "Path Following of Autonomous Vehicles in the Presence of Sliding Effects", IEEE Transactions on Vehicular Technology, vol. 61, no. 4, pp. 1481-1492, 2012.

[26] P. Falcone, F. Borrelli, H. Tseng, J. Asgari and D. Hrovat, "Linear time-varying model predictive control and its application to active steering systems: Stability analysis and experimental validation", International Journal of Robust and Nonlinear Control, vol. 18, no. 8, pp. 862-875, 2008.

[27] J. Ji, A. Khajepour, W. Melek and Y. Huang, "Path Planning and Tracking for Vehicle Collision Avoidance Based on Model Predictive Control With Multiconstraints", IEEE Transactions on Vehicular Technology, vol. 66, no. 2, pp. 952-964, 2017.

[28] C. Chen, Y. Jia, M. Shu and Y. Wang, "Hierarchical Adaptive Path-Tracking Control for Autonomous Vehicles", IEEE Transactions on Intelligent Transportation Systems, vol. 16, no. 5, pp. 2900-2912, 2015.

[29] H. Fang, L. Dou, J. Chen, et al, "Robust anti-sliding control of autonomous vehicles in presence of lateral disturbances", Control Engineering Practice, vol. 19, no. 5, pp. 468-478, 2011.

[30] C. Hu, R. Wang, F. Yan and H. Karimi, "Robust Composite Nonlinear Feedback Path-Following Control for Independently Actuated Autonomous Vehicles With Differential Steering", IEEE Transactions on Transportation Electrification, vol. 2, no. 3, pp. 312-321, 2016.

[31] C. Hu, R. Wang, F. Yan and N. Chen, "Robust Composite Nonlinear Feedback Path-Following Control for Underactuated Surface Vessels With Desired-Heading Amendment", IEEE Transactions on Industrial Electronics, vol. 63, no. 10, pp. 6386-6394, 2016.

[32] R. Lemos, O. Garcia, and J.V. Ferreira, "Local and global path generation for autonomous vehicles using splines", Ingeniería, 21(2), pp.188-200, 2016.

[33] Z. Liu, et al. "Robot path planning in impedance networks", Intelligent Control and Automation, WCICA 2006. The Sixth World Congress on. Vol. 2. IEEE, 2006.

[34] G. F. Marshall and L. Tarassenko, "Robot path planning using VLSI resistive grids", IEE Proceedings-Vision, Image and Signal Processing 141.4: 267-272, 1994.
[35] G. Cheng, M. Ikegami, and M. Tanaka, "A resistive mesh analysis method for parallel path searching", Circuits and Systems, Proceedings of the 34th Midwest Symposium on. IEEE, 1991.
[36] R. Rajamani, *Vehicle dynamics and control*, New York, NY, USA: Springer, 2012.
[37] W. Zhao, Fan Mili, Wang Chunyan. H∞/extension stability control of automotive active front steering system, Mechanical Systems and Signal Processing, 2019, 115: 621~636
[38] W. Zhao, Qin Xiaoxi, Wang Chunyan. Yaw and lateral stability control of Automotive four-wheel steer-by-wire system, IEEE/ASME Transactions on Mechatronics, Doi: 10.1109/TMECH.2018.2812220, 2018.
[39] Y. Zhang, Y. Huang, H. Wang and A. Khajepour, "A comparative study of equivalent modelling for multi-axle vehicle", Vehicle System Dynamics, vol. 56, no. 3, pp. 443-460, 2017.
[40] Y. Zhang, A. Khajepour and Y. Huang, "Multi-axle/articulated bus dynamics modeling: a reconfigurable approach", Vehicle System Dynamics, pp. 1-29, 2018.
[41] Jalali, Milad, et al. "Integrated stability and traction control for electric vehicles using model predictive control." *Control Engineering Practice* 54 (2016): 256-266.
[42] Borrelli, Francesco, et al. "MPC-based approach to active steering for autonomous vehicle systems." International Journal of Vehicle Autonomous Systems 3.2-4 (2005): 265-291.
[43] Borrelli, Francesco, Alberto Bemporad, and Manfred Morari. Predictive control for linear and hybrid systems. Cambridge University Press, 2017
[44] Y. Huang, H. Wang, A. Khajepour, H. He and J. Ji, "Model predictive control power management strategies for HEVs: A review", Journal of Power Sources, vol. 341, pp. 91-106, 2017.
[45] Y. Huang, A. Khajepour, T. Zhu, et al, "A Supervisory Energy-Saving Controller for a Novel Anti-Idling System of Service Vehicles", IEEE/ASME Transactions on Mechatronics, vol. 22, no. 2, pp. 1037-1046, 2017.
[46] J. Rossiter, Model-Based Predictive Control: A Practical Approach. CRC Press control series, CRC PressINC, 2003.
[47] Nahidi, Asal, et al. "Modular integrated longitudinal and lateral vehicle stability control for electric vehicles." Mechatronics 44 (2017): 60-70.

Yanjun Huang is a Research Associate at the Department of Mechanical and Mechatronics Engineering at University of Waterloo, where he received his PhD degree in 2016. His research interest is mainly on the vehicle holistic control in terms of safety, energy-saving, and intelligence, including vehicle dynamics and control, HEV/EV optimization and control, motion planning and control of connected and autonomous vehicles, human-machine cooperative driving.

He has published several books, over 50 papers in Journals and Conference. He is serving as the associate editor and editorial board member of IET Intelligent Transport System, SAE Int. J. of Commercial vehicles, Int. J. of Vehicle Information and Communications, Automotive Innovation, etc.

Haitao Ding received his Ph.D. in 2003 from the Jilin University. He is now a professor at the State Key Laboratory of Automotive Simulation & Control with the Jilin University. From 2015 to 2016, he had worked at University of Waterloo as a visiting professor.

His research interests include vehicle dynamics, automotive active safety control, electric vehicle simulation and control, and vehicle electronics. He has served as the PI or co-PI of more than 10 research projects such as 2 NSFC projects, 7 “863 Program” projects, one “973 Program”. He is the author of more than 30 publications.

Yubiao Zhang received the B.Sc. and M.Sc. degrees in mechanical engineering, specializing in vehicle mechatronics, from Hunan University, China, in 2012 and 2015.

He is currently pursuing the Ph.D. degree in mechanical engineering at the University of Waterloo, ON, Canada. His research interest includes the vehicle dynamics, reconfigurable control and optimization and automated driving.

Hong Wang is currently a Research Associate of Mechanical and Mechatronics Engineering with the University of Waterloo. She received her Ph.D. degree in Beijing Institute of Technology in China in 2015.

Her research focuses on the component sizing, modeling of hybrid powertrains and power management control strategies design for Hybrid electric vehicles; intelligent control theory and application; autonomous vehicles.

Dongpu Cao received the Ph.D. degree from Concordia University, Canada, in 2008. He is currently an Associate Professor at the University of Waterloo.

His research focuses on vehicle dynamics, control and intelligence, where he has contributed more than 150 publications, 1 book, and 1 US patent. He received the ASME AVTT’2010 Best Paper Award and 2012 SAE Arch T. Colwell Merit Award. Dr. Cao serves as an Associate Editor for IEEE Trans. on intelligent transportation systems, Vehicular Technology, Mechatronics, Industrial Electronics and ASME Journal of Dynamic systems, Measurement, and Control. He serves on the SAE International Vehicle Dynamics Standards Committee and a few ASME, SAE, IEEE technical committees.

Nan Xu is an associate professor at State Key Laboratory of Automotive Simulation and Control, Jilin University of China, where he received his Ph.D degree in 2012.

His current research focuses on tyre dynamics and tyre-road friction, dynamics and stability control of electric vehicles and autonomous vehicles.

Chuan Hu is currently a Postdoctoral Fellow at Department of Mechanical Engineering, University of Texas at Austin, Austin, USA. He received the Ph. D. degree in Mechanical Engineering, McMaster University, Hamilton, Canada in June 2017.

His research interest includes vehicle system dynamics and control, motion control and estimation of autonomous vehicles, robust and adaptive control. He has published over 20 journal papers on leading journals in automated vehicles areas, and is an editorial board member of the international journal Computer Simulation in Application, Journal of Advances in Vehicle Engineering, and a Guest Editor of Advances in Mechanical Engineering.